Article

Discovery Medicine 2026; 38(213): 3197–3207
https://doi.org/10.24976/Discov.Med.202638213.247

METTL3 Regulates ATIC Expression via m^{6}A Methylation: Implications for Methotrexate Action in Rheumatoid Arthritis

Baojing Zhao[1,†], Yuqian Miao[1,†], Xiudi Wu[1], Dongmei Xiao[1], Hua Huang[1], Tinghui Wang[1], Huyan Wang[1,*]

[1]Department of Rheumatology and Immunology, The First Affiliated Hospital of Ningbo University, 315010 Ningbo, Zhejiang, China
*Correspondence: wanghuyan_why123@163.com (Huyan Wang)
[†]These authors contributed equally.
Submitted: 9 July 2026 Revised: 5 August 2026 Accepted: 21 August 2026 Published: 23 October 2026

Background: Rheumatoid arthritis (RA), an autoimmune condition, causes fibroblast-like synoviocytes (FLSs) growth, joint inflammation, and erosion. Methotrexate (MTX), the principal treatment for this illness, has an unknown mechanism. We investigated the potential regulatory mechanism of MTX in RA-related synovial fibroblasts, focusing on whether MTX exerts therapeutic effects via regulating N6-methyladenosine (m^{6}A) modification mediated by methyltransferase like 3 (METTL3), which affects the expression of the key purine metabolism enzyme 5-Aminoimidazole-4-Carboxamide Ribonucleotide Formyltransferase/IMP Cyclohydrolase (ATIC).

Methods: The effects of MTX on RA-FLSs proliferation, migration, invasion, cell cycle distribution and apoptosis were assessed using methylthiazolyldiphenyl-tetrazolium bromide (MTT), Transwell assays and flow cytometry. METTL3 and ATIC protein levels were quantified by Western blotting. Functional rescue experiments were performed using METTL3-overexpressing cells, while the underlying molecular mechanism was investigated by methylated RNA immunoprecipitation (MeRIP) and RNA stability assays.

Results: RA-FLSs proliferation, migration, and invasion were significantly higher than those of normal FLSs ($p < 0.01$). The cells entered S phase, and apoptosis decreased. Meanwhile, METTL3 and ATIC protein expression levels were increased ($p < 0.01$). MTX suppressed RA-FLS proliferation and migration ($p < 0.01$), triggered G0/G1 phase arrest and apoptosis ($p < 0.001$), and decreased METTL3 and ATIC protein levels ($p < 0.05$). METTL3 overexpression restored ATIC protein expression ($p < 0.01$) and reversed MTX's cellular functional control on RA-FLSs ($p < 0.01$). METTL3 mediated m^{6}A modification of ATIC mRNA, which elevated the m^{6}A enrichment level of the ATIC transcript ($p < 0.001$) and slowed its mRNA degradation ($p < 0.05$).

Conclusion: MTX reduces m^{6}A enrichment in ATIC mRNA by suppressing METTL3, thereby decreasing ATIC expression. This METTL3-ATIC regulatory axis is associated with altered proliferation and apoptosis of RA-FLSs, suggesting a potential epitranscriptomic mechanism that may contribute to MTX's therapeutic effects. This study provides preliminary *in vitro* evidence for a novel molecular pathway underlying MTX activity in RA-related synovial fibroblasts and identifies directions for future mechanistic investigation in rheumatoid arthritis.

Keywords: RA; FLSs; MTX; METTL3; ATIC

Introduction

Approximately 0.5%–1% of the global population suffers from rheumatoid arthritis (RA), a chronic systemic autoimmune disease characterized bypersistent synovitis and joint erosion [1,2]. Although new therapies such as biological agents have continued to emerge, methotrexate (MTX) has remained the "anchor drug" for the treatment of RA since the late 1980s [3,4,5]. Its mechanism of action has not been fully clarified, and epigenetic regulation in particular has become an active area of research.

Genetic susceptibility and epigenetic regulatory abnormalities are critical to RA pathogenesis [6,7]. Single nucleotide polymorphisms (SNPs) in the 5-Aminoimidazole-4-Carboxamide Ribonucleotide Formyltransferase/IMP Cyclohydrolase (ATIC) gene are significantly associated with susceptibility to RA [8]. ATIC encodes an enzyme involved in the final step of the de novo purine synthesis pathway, catalyzingthe conversion of 5-aminoimidazole-4-formamide nucleotide (AICAR) to inosine monophosphate (IMP) [9]. Under pathological conditions in RA, the abnormal proliferation of fibroblast-like synoviocytes (FLSs) and immune cells sharply increases the demand for purine metabolism [10,11]. Abnormal ATIC activity may disrupt adenosine pathway homeostasis, enhance pro-inflammatory cytokine production and increase re-

Copyright: © 2026 The Author(s). Published by Discovery Medicine. This is an open access article under the CC BY 4.0 license.
Note: *Discovery Medicine* stays neutral with regard to jurisdictional claims in published maps and institutional affiliations.

sistance to apoptosis in synovial cells. It is worth noting that after MTX is converted into the active metabolite MTX-polyglutamic acid (MTX-PGs) in cells, it can efficiently inhibit ATIC enzyme activity, and this inhibitory effect is significantly stronger than that on dihydrofolate reductase (DHFR) [12,13]. This characteristic suggests that ATIC may be an important metabolic target through which MTX exerts its anti-rheumatic effect; however, the epigenetic mechanism by which MTX regulates ATIC have not been fully clarified. Animal experiments have shown that MTX treatment can lead to abnormal accumulation of ATIC proteins in mouse tissues, accompanied by increased extracellular adenonucleotide levels, thereby exerting anti-inflammatory effects through activation of adenosine A2A receptors [14]. These findings indicate that the regulation of ATIC by MTX may involve multiple mechanisms.

Epigenetic modifications, particularly RNA methylation, provide a novel perspective for elucidating the mechanisms underlying MTX action. N6-methyladenosine (m^6A) is the predominant internal modification of eukaryotic mRNA, and its dynamic regulation is jointly mediated by methyltransferase complexes (e.g., methyltransferase like METTL3, METTL14) [15,16,17], demethylases (e.g., alkylation repair homolog 5) [18] and methyl recognition proteins (e.g., YTH N6-methyladenosine RNA binding proteins) [19]. These regulators are widely involved in processes such as immune cell differentiation, inflammatory factor expression, and tissue repair. In the pathological microenvironment of RA, pro-inflammatory cytokines including tumor necrosis factor-α (TNF-α) can significantly up-regulate m^6A modification and METTL14 in FLSs, suggesting that the m^6A methylation pathway may drive RA progression by regulating the post-transcriptional metabolism of inflammation-related genes [17].

Previous studies have found that MTX intervention can dose-dependently reduce the overall level of m^6A modification in FLSs and inhibit METTL3 protein expression, suggesting that MTX may exert its effect through epigenetic regulatory pathways. Given the role of ATIC as an RA susceptibility gene and its direct interaction with MTX, this study proposes that MTX may regulate ATIC mRNA stability and protein expression by inhibiting METTL3-catalyzed m^6A methylation.

Materials and Methods

Cell Culture

Human normal synovial fibroblasts (FLSs, CP-H241, Pricella, Wuhan, China) were identified by short tandem repeat. The cell line used in this study were tested for mycoplasma contamination prior to experimental use, and all test results were negative. FLSs was cultured in human synovial fibroblast complete medium (CM-H241, Pricella, Wuhan, China). Then the cells were placed in a 37 °C incubator (Forma Steri-Cult, ThermoFisher, Waltham, MA, USA) containing 5% CO_2 for culture.

Cell Models and Grouping

Based on previous research, an RA cell model was established by culturing FLSs with 100 ng/mL TNF-α for 3 h [20]. In subsequent experiments, the RA model cells were designated as RA-FLSs. Log-phase cells were collected, plated, and assigned into FLSs, RA-FLSs and RA-FLSs+MTX groups. Cells in the FLSs and RA-FLSs groups were routinely cultured, while RA-FLSs in the RA-FLSs+MTX group were treated with 0.01 μg/mL MTX (HY-14519, MCE, Monmouth Junction, NJ, USA) during culture [21]. Then, all groups of cells were placed in the incubator for a 48-h incubation period and then harvested for subsequent experiments.

Next, transfection of METTL3 overexpression plasmid in RA-FLSs was carried out. Lentiviral vector for Human METTL3 gene expression (pLV [Exp]-EGFP/Puro-EF1A>hMETTL3 [NM_019852.5]) and its negative control (NC) were procured from Yunzhou Biosciences (Guangzhou). The viral titer was 1×10^8 TU/mL. RA-FLSs were seeded at 3×10^5 cells/well in 6-well plates and infected at MOI = 20 in complete medium containing 5 μg/mL Polybrene (sc-134220, Santa Cruz, Dallas, TX, USA) for 12 hours. Stable cell lines were selected with 2 μg/mL puromycin (A1113803, Gibco, Waltham, MA, USA) for 7 days, beginning 48 hours post-infection. Transfection efficiency in RA-FLSs was detected by quantitative real-time polymerase chain reaction (qRT-PCR) 48 h post-transfection with overexpression plasmids/NC. Then cells were allocated into 4 groups: Control (conventional culture); MTX (0.01 μg/mL MTX added during culture); MTX+NC (0.01 μg/mL MTX added after transfection with NC); MTX+METTL3 (METTL3 overexpression plasmid transfection and culture with 0.01 μg/mL MTX). Cells in each group were cultured for 48 h, and the cells were then collected for subsequent experiments, including cell viability, migration, apoptosis and protein detection.

Methylthiazolyldiphenyl-tetrazolium Bromide (MTT) Assay

Cells under optimal growth conditions were injected into 96-well plates (FCP962, Beyotime, Shanghai, China) (5000/well), cultured for 24 h, and treated in accordance with grouping (48 h). Then MTT (10 μL; C0009S, Beyotime, Shanghai, China) was added to each well and incubated for 4 h. Following culture with dimethyl sulfoxide (DMSO, 150 μL; HY-Y0320C, MCE, Monmouth Junction, NJ, USA), the absorbance was measured at 570 nm utilizing a multifunctional enzyme marker (Varioskan LUX, Thermo Fisher, Waltham, MA, USA).

Colony Formation Experiment

After precipitation, the cells were counted, diluted to 1×10^3 cells/mL, and seeded in to six-well plates (200/well; FCP060, Beyotime, Shanghai, China). After cell adhesion, treatment was performed according to the experi-

mental groups, and the cells were cultured for 2–3 weeks. When distinct colonies became visible, the culture was terminated, the medium was removed, and the plates were gently washed two to three times with phosphate buffered saline (PBS, ST477, Beyotime, Shanghai, China). The cells were fixed with 1 mL methanol (C06901102, Nanjing Reagent, Nanjing, China) for 15-min and then stained with 1 mL Giemsa dye (C0133, Beyotime, Shanghai, China) for 30 min. The staining solution was gently removed under running water, and the colonies were counted and documented using a microscope (THUNDER Imager Tissue, Leica, Wetzlar, Germany).

Transwell Assay

Before the experiment, the Matrigel matrix gel (40183ES08, Yeasen, Shanghai, China) was diluted 1:8 with serum-free medium. After preparation on ice, 50 µL was used to coat the inner surface of the Transwell insert membrane (3462, Corning, NY, USA), and incubated at 37 °C for 3 h to form a gel for the invasion assays, thereby simulating the extracellular matrix. The migration experiment did not require coating. A total of 5×10^4 cells were suspended in 200 µL serum-free medium, and the cell suspension was added to the apical (upper) chamber. Then, 600 µL of medium containing 10% FBS was added to the basal (lower) chamber, and the cells were incubated at 37 °C for 48 h. The inserts were then removed, rinsed with PBS, fixed with 4% paraformaldehyde (PFD, abs9179, Absin, Shanghai, China) for 20 min, stained with 0.1% crystal violet (C0121, Beyotime, Shanghai, China) for 15 min, and rinsed with distilled water. Cells that had not migrated or invaded through the membrane were gently removed from the upper surface with a cotton swab. Five fields were randomly photographed under a microscope at 200× magnification, and the transmembrane cells were counted to evaluate migration and invasion abilities. During the procedure, Matrigel was kept on ice to prevent coagulation, and gentle rinsing was performed after staining to prevent cell detachment.

Flow Cytometry

After collection and washing, cells were suspended in 600 µL buffer, incubated with 5 µL Annexin V-fluorescein isothiocyanate (FITC) and 10 µL propidium iodide (PI, C1062S, Beyotime, Shanghai, China), and underwent apoptosis assessment using FACSCalibur flow cytometry (BD Biosciences, Franklin Lakes, NJ, USA). 70% ethanol (C06915550, Nanjing Reagent, Nanjing, China) was used to immobilise the cells, and they were then re-suspended in PBS. Then, the cells were treated with 100 µg/mL RNase A (ST576, Beyotime, China) and incubated at 37 °C for 30 minutes to ensure complete RNA degradation. The cells were then treated again with 50 µg/mL PI and 0.2% Triton X-100 (P0096, Beyotime, Shanghai, China) at 4 °C for 0.5 h, and the cell-cycle distribution was analyzed by flow cytometry.

Western Blot

Cellular proteins were isolated using radioimmunoprecipitation buffer (RIPA, PC901, Biomiga, San Diego, CA, USA), and protein detection was performed with the help of the bicinchoninic acid assay (BCA) kit (KGP903, KeyGEN, Nanjing, China). Sodium dodecyl sulfate-polyacrylamide gel electrophoresis (SDS-PAGE, P0012A, Beyotime, Shanghai, China) was used to separate the proteins. Subsequently, the polyvinylidene fluoride (PVDF) membrane (2215, Millipore, Burlington, MA, USA) was placed in 5% skimmed milk, shaken, and sealed at 37 °C for 120 min. The membranes were incubated overnight with the primary antibody at 4 °C (Table 1), and then with goat anti-rabbit /goat anti mouse antibodies at room temperature (Table 1). Finally, the bands were visualized using an iBright CL750 (Thermo Fisher, Waltham, MA, USA) with ECL reagent (P0018FS, Beyotime, Shanghai, China), and glyceraldehyde-3-phosphate dehydrogenase (GAPDH) served as the endogenous control. Band intensities were quantified using ImageJ software (version 1.53t, NIH, MD, USA). Regions of interest (ROIs) of identical dimensions were drawn around each target band, and integrated optical density (IOD) was measured after background subtraction. Relative protein expression was calculated by normalizing the IOD of the target protein to that of GAPDH in the same lane.

qRT-PCR

First, cellular RNA was obtained using Trizol reagent (R0016, Beyotime, Shanghai, China). Subsequently, cDNA was prepared using the High Capacity cDNA Reverse Transcription Kit (4368813, Applied Biosystems, Foster City, CA, USA). cDNA amplification was performed with SYBR Green qPCR Mix (D7265, Beyotime, Shanghai, China) and C1000 Touch™ PCR instrument (E1138, Bio-rad, Hercules, CA, USA). GAPDH served as the endogenous reference, and relative expression levels were calculated using the $2^{-\Delta\Delta Ct}$ method. The primer information is shown in Table 2, and the primerswere synthesized by Tsingke (Beijing, China).

Methylated RNA Immunoprecipitation (MeRIP)

According to the method specified in the instructions of the m^6A MeRIP Kit (C11051-1, RIBOBIO, Guangzhou, China), total RNA of cells was extracted. For each reaction, 5 µg of m^6A antibody (mouse monoclonal, provided in the kit) or 5 µg of negative control IgG (mouse normal IgG, provided in the kit) was added to the immunoprecipitation (IP) buffer and incubated with 50 µL protein A/G magnetic beads for 1 hour. A total of 20 µg RNA was used per IP reaction, of which 10% (2 µg) was reserved as Input control. Then, the RNA samples and the antibody-conjugated magnetic beads were resuspended in IP buffer and incubated overnight at 4 °C. RNA was eluted using the elution buffer. After extraction and purifica-

Table 1. Antibodies used in this study.

Name	Catalog	Molecular weight (kDa)	Dilution	Manufacturer (UK)
METTL3	ab195352	64	1/1000	abcam
ATIC	ab188321	65	1/1000	abcam
GAPDH	ab8245	36	1/10,000	abcam
goat anti mouse	ab205719	—	1/2000	abcam
goat anti rabbit	ab205718	—	1/2000	abcam

METTL3, methyltransferase like 3; ATIC, 5-Aminoimidazole-4-Carboxamide Ribonucleotide Formyltransferase/IMP Cyclohydrolase; GAPDH, glyceraldehyde-3-phosphate dehydrogenase.

Table 2. Gene sequence primers.

Name	Forward primer(5'-3')	Reverse primer(5'-3')
METTL3	TCAGCATCGGAACCAGCAAA	TGGGGATTTCCTTTGACACCA
ATIC	AGCAAGAGGGGCTGATAGGA	AATCAGTGGTGGAAGAGCCG
GAPDH	TGCACCACCAACTGCTTAGC	GGCATGGACTGTGGTCATGAG

tion with phenol (C04801102, Nanjing Reagent, Nanjing, China)-chloroform (C07615202, Nanjing Reagent, Nanjing, China), it was analyzed by qRT-PCR (primer sequences shown in Table 2). For qPCR analysis, both Input (10% of total RNA) and IgG controls were included. The m^6A enrichment level was calculated using the percent Input method: $\%Input = 2^{Ct_Input - Ct_IP} \times Dilution\ Factor \times 100\%$.

RNA Stability Experiment

Actinomycin D (ActD) is an inhibitor of DNA transcription and replication. Cells in the NC and METTL3 groups were treated with ActD (5 μmol/L, HY-17559, MCE, Monmouth Junction, NJ, USA) [22], and cellular RNA was collected at 0, 2, 4, 6, and 8 h after treatment. Changes in RNA expression were detected by qRT-PCR.

Statistical Analysis

Statistical analysis was conducted with GraphPad Prism 8.0 (GraphPad Software, San Diego, CA, USA). Prior to parametric testing, normality of distribution was assessed by the Shapiro-Wilk test and homogeneity of variances by Levene's test; all datasets met the assumptions for parametric analysis. For comparisons across three or more groups, one-way analysis of variance (ANOVA) was used, followed by Tukey's HSD post-hoc test for pairwise multiple comparisons when the overall ANOVA was significant. For the RNA stability analysis, two-way ANOVA was performed with time and group as independent variables, followed by Tukey's multiple comparisons test. $p < 0.05$ was considered statistically significant. Data are presented as the mean ± standard deviation.

Results

MTX Decreased RA-FLS Proliferation and Migration, Suppressed the Expression of METTL3 and ATIC Proteins, and Induced Cell Death.

First, we verified the effect of MTX on fibroblast-like synovial cells. Compared with the FLSs cells in the control group, the viability (Fig. 1A), proliferation (Fig. 1B,C), migration and invasion abilities (Fig. 1D–F) of RA-FLSs were significantly enhanced ($p < 0.01$). However, MTX attenuated these cell biological activities (Fig. 1A–F, $p < 0.01$). Flow cytometry results showed that, compared with FLSs, the proportion of RA-FLSs in the G0/G1 phase was decreased, whereas the proportion in the S phase was significantly increased (Fig. 2A,B, $p < 0.001$). MTX treatment induced cell arrest in the G0/G1 phase (Fig. 2A,B, $p < 0.001$). The proportion of cells in the G0/G1 phase was higher in the RA-FLSs+MTX group than in the RA-FLSs group, whereas the proportion in the S phase was lower (Fig. 2A,B, $p < 0.001$). Furthermore, our results confirmed that MTX induced apoptosis in RA-FLSs (Fig. 2C,D, $p < 0.001$). METTL3 and ATIC protein levels were higher in the RA-FLSs group than in the FLSs group and were reduced following MTX treatment (Fig. 2E–G, $p < 0.05$).

MTX Regulated RA-FLS Proliferation, Migration and Apoptosis Through METTL3

To verify the role of METTL3 in the treatment of rheumatoid arthritis by MTX, we established a RA-FLSs cell line with *METTL3* overexpression (Fig. 3A, $p < 0.001$). In the following experiments, we treated RA-FLSs with MTX or administered MTX after transfection with the METTL3 overexpression plasmid. Furthermore, MTX treatment significantly inhibited cell viability, proliferation, migration, and invasion (Fig. 3B–G, $p < 0.001$), while METTL3 overexpression offset these effects of MTX on the cells (Fig. 3B–G, $p < 0.01$). Next, we also assessed cell

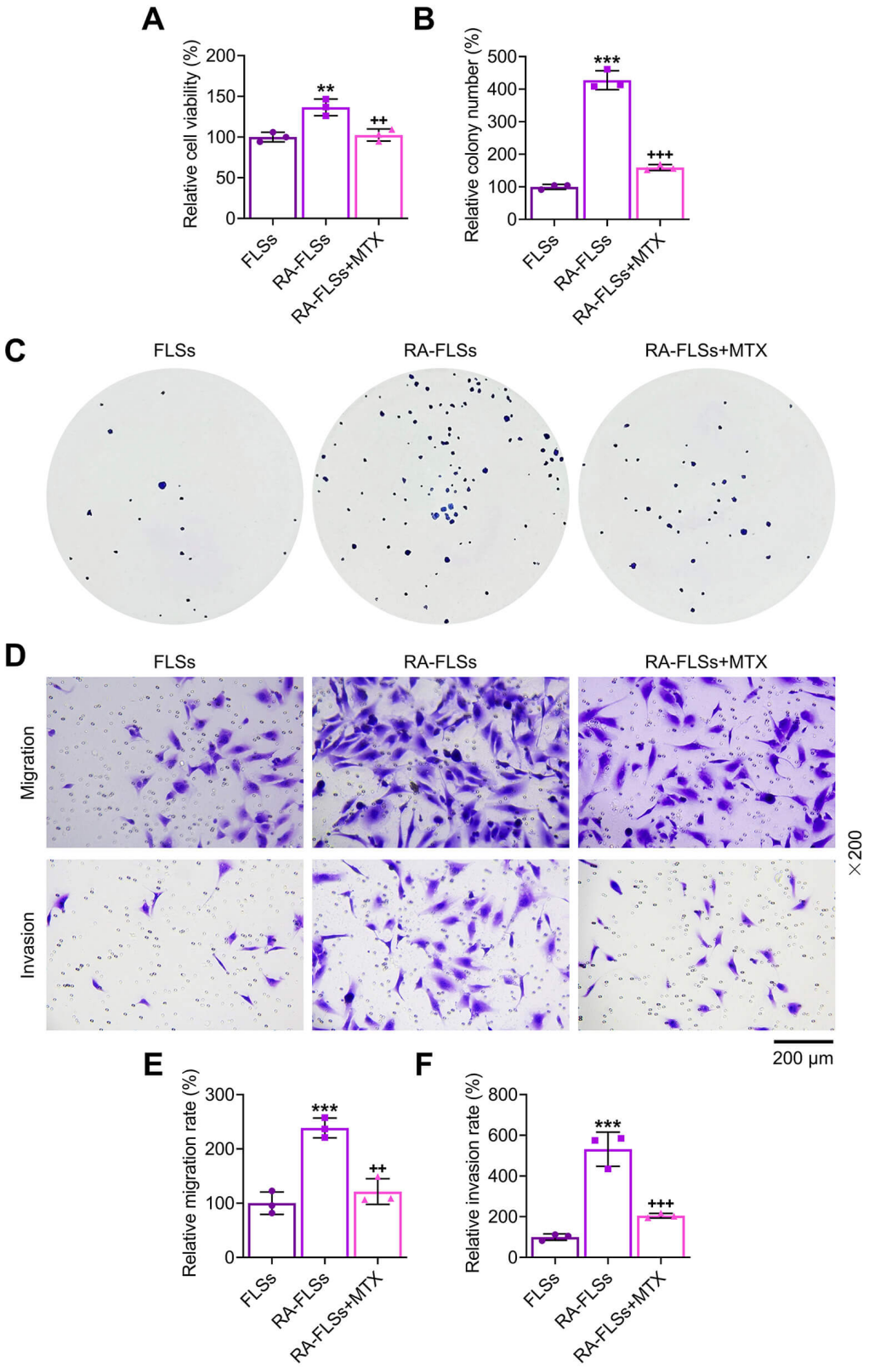


Fig. 1. Methotrexate (MTX) inhibited RA-FLS activity, proliferation, migration and invasion. (A) Cell activity (Methylthiazolyldiphenyl-tetrazolium bromide (MTT)). (B,C) Cell proliferation (clone formation assay). (D–F) Cell migration and invasion (Transwell assay). Magnification: 200×, bar: 200 μm. Each group of experiments was repeated thrice (n = 3). $^{**}p < 0.01$, $^{***}p < 0.001$ vs. FLSs; $^{++}p < 0.01$, $^{+++}p < 0.001$ vs. RA-FLSs.

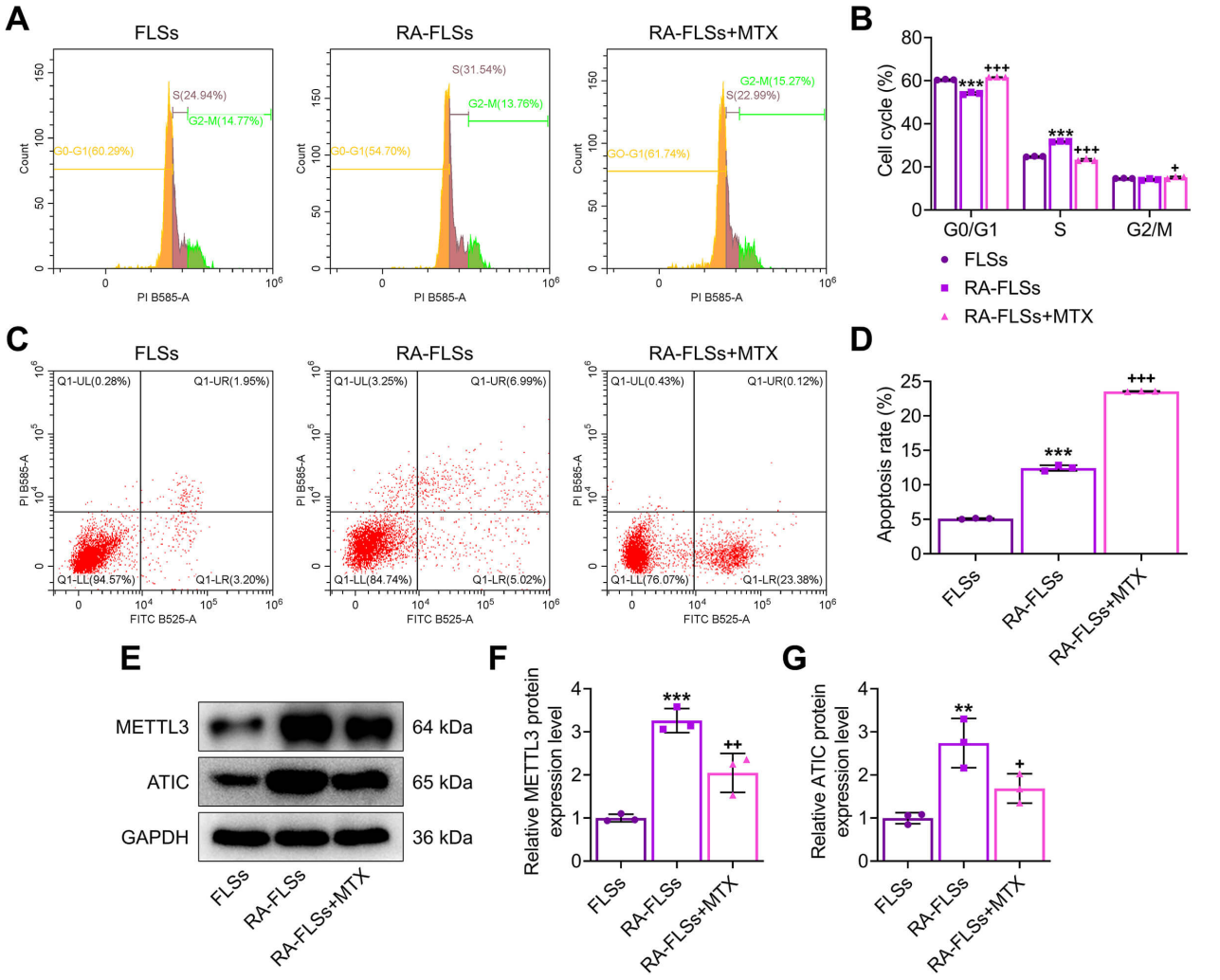


Fig. 2. MTX induced cell arrest in the G0/G1 phase of RA-FLSs, promoted cell apoptosis, and down-regulated methyltransferase like 3 (METTL3) and 5-Aminoimidazole-4-Carboxamide RibonucleotideFormyltransferase/IMP Cyclohydrolase (ATIC) proteins. (A,B) Cell cycle (flow cytometry). (C,D) Cell apoptosis (flow cytometry). (E–G) METTL3 and ATIC expressions (Western blot; Glyceraldehyde-3-phosphate dehydrogenase (GAPDH) as internal parameter). Each group of experiments was repeated thrice (n = 3). $^{**}p < 0.01$, $^{***}p < 0.001$ vs. FLSs; $^{+}p < 0.05$, $^{++}p < 0.01$, $^{+++}p < 0.001$ vs. RA-FLSs.

cycle distribution and apoptosis. MTX treatment increased the G0/G1 phase population and decreased the S phase population (Fig. 4A,C, $p < 0.001$). Conversely, METTL3 overexpression counteracted the effect of MTX, decreasing G0/G1 fraction and increasing the S phase proportion (Fig. 4A,C, $p < 0.001$). Moreover, MTX treatment promoted apoptosis of RA-FLSs, while METTL3 overexpression reversed the effects of MTX and inhibited apoptosis (Fig. 4B,D, $p < 0.001$). In addition, MTX reduced ATIC protein levels in cells, while METTL3 overexpression reversed this inhibitory effect (Fig. 4E,F, $p < 0.01$).

METTL3 Stabilized ATIC via m^{6}A Modification of the ATIC Transcript

To explore whether METTL3 participates in modulating m^{6}A modification of ATIC mRNA, we performed MeRIP-qPCR assay with m6A antibody enrichment to measure the total m6A enrichment of ATIC transcripts. The m^{6}A level of ATIC increased following METTL3 overexpression (Fig. 4G, $p < 0.001$). These data supported the involvement of METTL3 in m^{6}A modification of ATIC mRNA. We next performed mRNA decay assays to clarify the effects of METTL3 on ATIC transcript abundance. After METTL3 overexpression, cells were treated with 5 µmol/L Act-D (an RNA synthesis inhibitor) for gradient time points, and *ATIC* mRNA levels were quantified via qRT-PCR. METTL3 overexpression slowed the degradation of *ATIC* mRNA (Fig. 4H). At 8 h, *ATIC* mRNA expression in the METTL3 group was higher than that in the NC group (Fig. 4H, $p < 0.05$). Collectively, METTL3 could stabilize *ATIC* transcripts by regulating the overall m^{6}A modification level of *ATIC* mRNA.

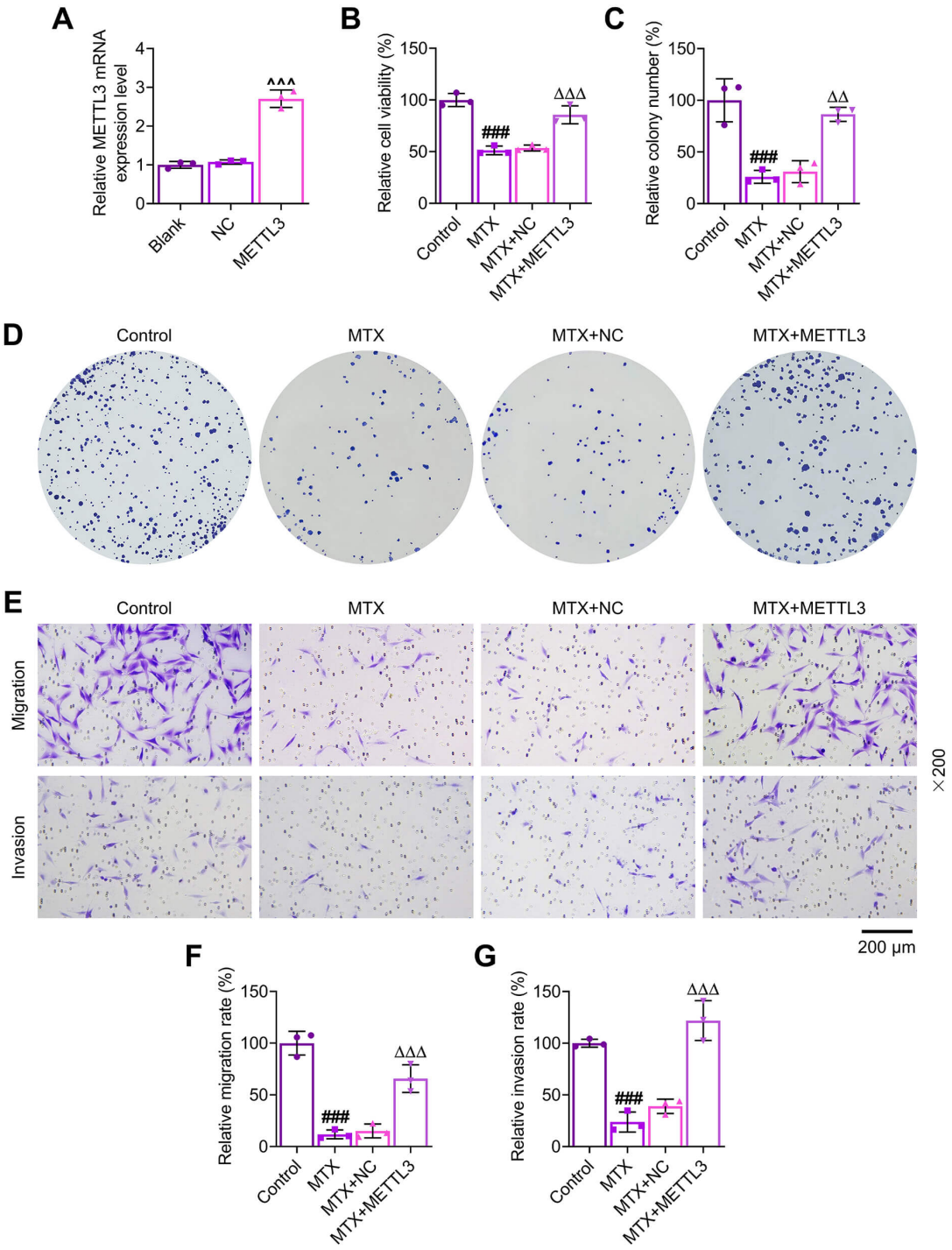


Fig. 3. METTL3 overexpression reversed the effects of MTX on the viability, proliferation, migration and invasion of RA-FLSs. (A) Transfection efficiency of *METTL3* overexpression plasmids (quantitative real-time polymerase chain reaction (qRT-PCR), GAPDH as internal parameter). (B) Cell activity (MTT). (C,D) Cell proliferation (clone formation assay). (E–G) Cell migration and invasion (Transwell assay). Magnification: 200×, bar: 200 μm. Each group of experiments was repeated thrice (n = 3). $^{\wedge\wedge\wedge}p < 0.001$ vs. Negative control (NC); $^{\#\#\#}p < 0.001$ vs. Control; $^{\Delta\Delta}p < 0.01$, $^{\Delta\Delta\Delta}p < 0.001$ vs. MTX+NC.

Discussion

The pathogenesis of RA involves a complex network of abnormal activation of immune cells, excessive proliferation of synovial cells and inflammatory imbalance of the joint microenvironment [23,24]. As an "anchor drug" for the treatment of RA, MTX can inhibit glucocorticoid-induced osteoclast generation by activating the IFN-γR/STAT1 pathway to treat RA [25], but its role in epigenetic regulation still needs to be further investigated.

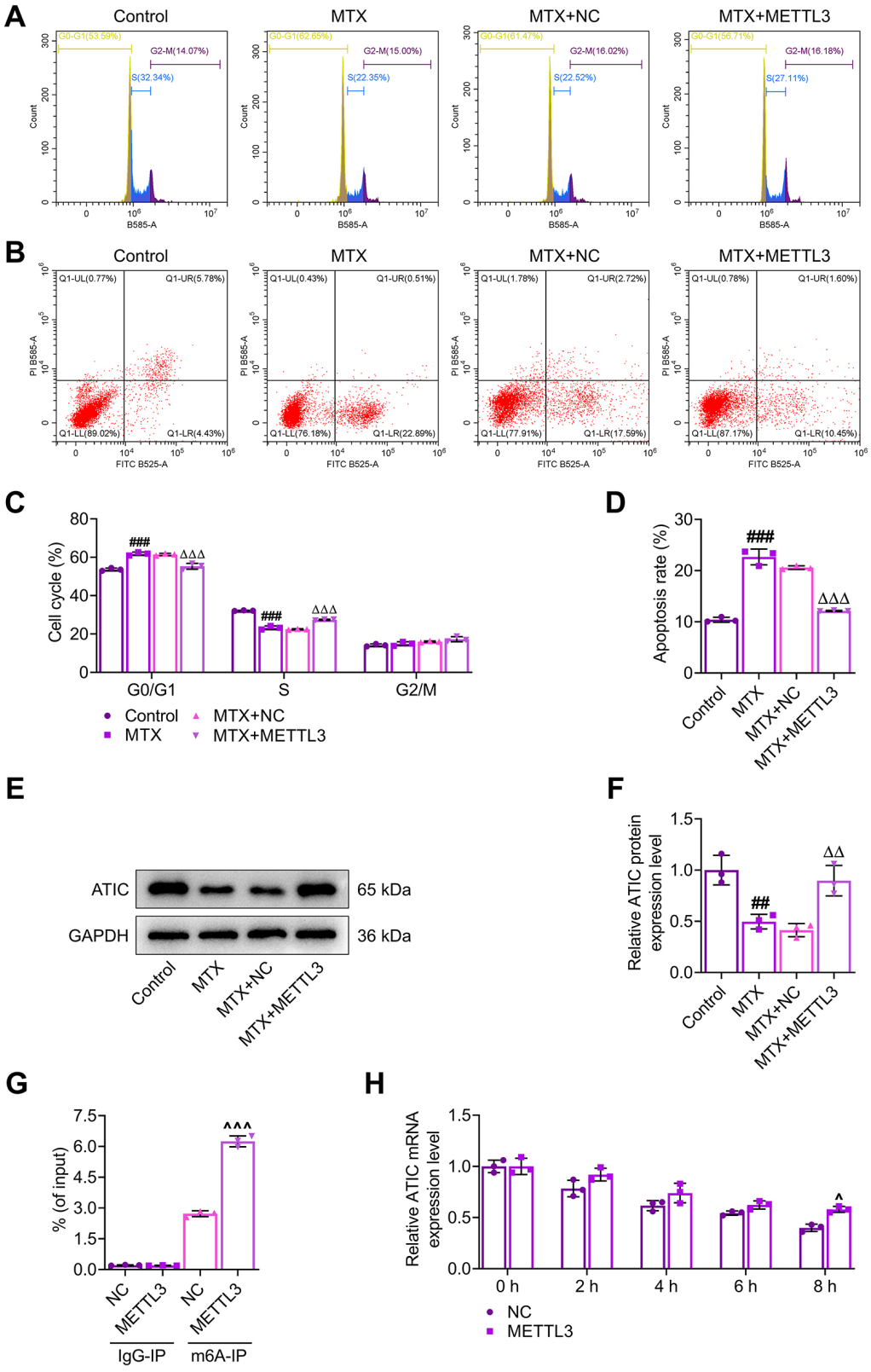


Fig. 4. METTL3 overexpression reversed the effects of MTX on cell cycle distribution, apoptosis and protein expression in RA-FLSs. (A,C) Cell cycle (flow cytometry). (B,D) Cell apoptosis (flow cytometry). (E,F) ATIC expression (Western blot, GAPDH as internal parameter). (G) Influence of METTL3 overexpression on the m^{6}A level of ATIC (Methylated RNA immunoprecipitation (MeRIP)). (H) Effect of METTL3 overexpression on *ATIC* decay (qRT-PCR). Each group of experiments was repeated thrice (n = 3). $^{\#\#}p < 0.01$; $^{\#\#\#}p < 0.001$ vs. Control; $^{\Delta\Delta}p < 0.01$, $^{\Delta\Delta\Delta}p < 0.001$ vs. MTX+NC; $^{\wedge}p < 0.05$, $^{\wedge\wedge\wedge}p < 0.001$ vs. NC.

In recent years, the regulatory functions of RNA methylation modifications (such as m^6A) in inflammatory diseases have gradually been revealed [26]. In the present *in vitro* study, we explored the effect of MTX on the METTL3/ATIC/m^6A axis in RA-FLSs, which provides a preliminary cellular perspective for understanding the potential regulatory mechanism of MTX in RA-related synovial fibroblasts.

The abnormal proliferation, migration and invasion of RA-FLSs are key driving factors of joint erosion, and their uncontrolled growth is closely related to abnormal cell cycle regulation and apoptosis resistance [27]. This study found that MTX could significantly repress RA-FLS viability, proliferation and migration, induce cell cycle arrest at the G0/G1 phase and promote apoptosis. It is worth noting that the expression levels of METTL3 and ATIC proteins in RA-FLSs were significantly higher than those in normal synovial cells, while MTX intervention could down-regulate the levels of both. As the core component of the m^6A methyltransferase complex [28], METTL3, overexpression can reverse the inhibitory effect of MTX on proliferation and its apoptosis-inducing effect in RA-FLSs, suggesting that METTL3 is a key molecular node through which MTX exerts its anti-synovitis effect. Notably, all MTX-treated groups had identical folate and purine metabolic suppression. Ectopic METTL3 overexpression partially rescued cell phenotypes and ATIC expression under continuous MTX exposure. As metabolic inhibition remained constant, the rescue effect was attributable to METTL3-dependent m6A regulation, allowing us to distinguish MTX's canonical metabolic action from this independent epitranscriptomic pathway.

A study on arthritis has shown that high METTL3 expression may continuously activate the pro-inflammatory phenotype in osteoarthritis mice by maintaining the stability of m^6A-modified inflammation-related genes [29]. Consistent with these findings, our data showed that METTL3 overexpression rescued the migratory capacity of RA-FLSs and reversed MTX-induced cell cycle arrest. These observations suggest that the METTL3/m6A cascade represents a potential regulatory branch mediating MTX function and may help elucidate the epitranscriptomic effects of MTX. As the terminal enzyme of the purine synthesis pathway, abnormal ATIC expression is strongly associated with genetic susceptibility to RA [8,30]. Our results showed that ATIC protein abundance was partially recovered upon METTL3 overexpression. Further mRNA decay assays verified that METTL3 slowed ATIC transcript degradation by modulating the overall m^6A modification level of ATIC mRNA. MeRIP-qPCR results further confirmed that METTL3 elevated the global m6A enrichment of ATIC transcripts, thereby hampering their degradation. Excessive activation of ATIC in RA can lead to an imbalance in adenonucleotide metabolism and the release of pro-inflammatory factors. Herein, we demonstrated that MTX suppresses METTL3 expression, thereby reducing the overall m^6A modification level of ATIC mRNA, accelerating ATIC mRNA degradation, and limiting overactive purine synthesis in RA-FLSs. This epitranscriptomic cascade may represent an auxiliary cellular mechanism by which MTX modulates purine metabolic enzyme expression in synovial fibroblasts. Whether this *in vitro* observation contributes to the clinical reduction of serum uric acid during MTX treatment [31] remains to be validated in patient cohorts. Our findings provide preliminary experimental evidence supporting a potential crosstalk network between purine metabolism and epitranscriptomic regulation in the cellular context of RA pathogenesis.

Previous research on MTX for RA has primarily focused on clinical trials. Clinical studies have demonstrated that Janus Kinase (JAK) inhibitors combined with MTX improve RA remission [32]. The present *in vitro* study characterizes an additional cellular biological effect of MTX on RA-FLSs and identifies a potential epitranscriptomic route through which MTX regulates RA-FLSs proliferation and ATIC-mediated purine metabolic homeostasis via the METTL3/m6A cascade. Our data provide preliminary molecular evidence that MTX modulates RA-FLSs behavior through epitranscriptomic mechanisms *in vitro*.

However, this study has several limitations. First, the METTL3/ATIC/m^6A axis was examined only *in vitro* and was not validated in an RA animal model. Second, MeRIP-qPCR was used only to assess the overall m^6A enrichment of ATIC mRNA, and the specific m^6A modification sites were not identified. Third, only METTL3 overexpression assays were performed, without complementary knockdown experiments to further verify the METTL3-ATIC regulatory relationship.

Conclusion

This study revealed that MTX downregulates METTL3, thereby reducing m^6A enrichment on ATIC mRNA and ATIC expression, which is associated with changes in RA-FLS proliferation and apoptosis. Future studies should validate this axis in RA animal models, identify functional m^6A sites on ATIC through sequencing and site-directed mutagenesis, perform complementary METTL3 knockdown experiments to further confirm the METTL3-ATIC regulatory relationship, and explore the potential therapeutic effects of combining METTL3 inhibitors with MTX for RA treatment.

Availability of Data and Materials

The datasets used or analyzed during the current study are available from the corresponding author upon reasonable request.

Author Contributions

BJZ, YQM and XDW designed the research study; DMX and HH performed the research; THW and HYW collected and analyzed the data. HYW has been involved in drafting the manuscript and all authors have been involved in revising it critically for important intellectual content. All authors gave final approval of the version to be published. All authors have participated sufficiently in the work to take public responsibility for appropriate portions of the content and agreed to be accountable for all aspects of the work in ensuring that questions related to its accuracy or integrity.

Ethics Approval and Consent to Participate

Not applicable.

Acknowledgment

Not applicable.

Funding

This work was supported by the Zhejiang Provincial Medical and Health Science and Technology Plan [grant number: 2024KY1510].

Conflict of Interest

The authors declare no conflict of interest.

References

[1] Venetsanopoulou AI, Alamanos Y, Voulgari PV, Drosos AA. Epidemiology of rheumatoid arthritis: genetic and environmental influences. Expert Review of Clinical Immunology. 2022; 18: 923–931. https://doi.org/10.1080/1744666X.2022.2106970

[2] Radu AF, Bungau SG. Management of Rheumatoid Arthritis: An Overview. Cells. 2021; 10: 2857. https://doi.org/10.3390/cells10112857

[3] Zhao Z, Hua Z, Luo X, Li Y, Yu L, Li M, et al. Application and pharmacological mechanism of methotrexate in rheumatoid arthritis. Biomedicine & Pharmacotherapy = Biomedecine & Pharmacotherapie. 2022; 150: 113074. https://doi.org/10.1016/j.biopha.2022.113074

[4] Torres RP, Santos FP, Branco JC. Methotrexate: Implications of pharmacogenetics in the treatment of patients with Rheumatoid Arthritis. ARP Rheumatology. 2022; 1: 225–229.

[5] Alharthi A, Magadmi R, Jamal M. Polymorphisms for the Clinical Efficacy and Toxicity of Methotrexate in Patients with Rheumatoid Arthritis: Systemic Review. International Journal of Pharmacology. 2024; 20: 547–551. https://doi.org/10.3923/ijp.2024.547.551

[6] Chen L, Wu B, Mo L, Chen H, Zhao Y, Tan T, et al. Associations between biological ageing and the risk of, genetic susceptibility to, and life expectancy associated with rheumatoid arthritis: a secondary analysis of two observational studies. The Lancet. Healthy Longevity. 2024; 5: e45–e55. https://doi.org/10.1016/S2666-7568(23)00220-9

[7] Huang C, Liang Y, Li Y, Wei Q, Ouyang L, Zhang J. The epigenetic landscape of rheumatoid arthritis: Pathogenesis and drug therapeutic potentials. Acta Pharmaceutica Sinica. B. 2025; 15: 5601–5631. https://doi.org/10.1016/j.apsb.2025.08.022

[8] Gallardo-Moya SG, Gonzalez-Lopez L, Contreras-Haro B, Mireles-Ramirez MA, Villagomez-Vega A, Morán-Moguel MC, et al. Genetic Variants of the *ATIC* Gene and Therapeutic Response to Methotrexate in Patients with Rheumatoid Arthritis. International Journal of Molecular Sciences. 2025; 26: 4013. https://doi.org/10.3390/ijms26094013

[9] Wizrah MSI, Chua SMH, Luo Z, Manik MK, Pan M, Whyte JML, et al. AICAR transformylase/IMP cyclohydrolase (ATIC) is essential for de novo purine biosynthesis and infection by Cryptococcus neoformans. The Journal of Biological Chemistry. 2022; 298: 102453. https://doi.org/10.1016/j.jbc.2022.102453

[10] Falconer J, Murphy AN, Young SP, Clark AR, Tiziani S, Guma M, et al. Review: Synovial Cell Metabolism and Chronic Inflammation in Rheumatoid Arthritis. Arthritis & Rheumatology (Hoboken, N.J.). 2018; 70: 984–999. https://doi.org/10.1002/art.40504

[11] Cao S, Li Y, Song R, Meng X, Fuchs M, Liang C, et al. L-arginine metabolism inhibits arthritis and inflammatory bone loss. Annals of the Rheumatic Diseases. 2024; 83: 72–87. https://doi.org/10.1136/ard-2022-223626

[12] Yamamoto T, Shikano K, Nanki T, Kawai S. Folylpolyglutamate synthase is a major determinant of intracellular methotrexate polyglutamates in patients with rheumatoid arthritis. Scientific Reports. 2016; 6: 35615. https://doi.org/10.1038/srep35615

[13] Abdallah HY, Ibrahim ME, Abd El-Fadeal NM, Ali DA, Elsehrawy GG, Badr RE, et al. Pharmacogenomics of Methotrexate Pathway in Rheumatoid Arthritis Patients: Approach toward Personalized Medicine. Diagnostics (Basel, Switzerland). 2022; 12: 1560. https://doi.org/10.3390/diagnostics12071560

[14] You X, Williams A, Dervieux T, He W, Cronstein BN. Fibroblasts from methotrexate-sensitive mice accumulate methotrexate polyglutamates but those from methotrexate-resistant mice do not. Clinical and Experimental Rheumatology. 2013; 31: 433–435.

[15] Su Y, Wu Z, Liu Y, Liu X, Kang J, Jia J, et al. Increased m6A RNA methylation and METTL3 expression may contribute to the synovitis progression of rheumatoid arthritis. Experimental Cell Research. 2024; 442: 114237. https://doi.org/10.1016/j.yexcr.2024.114237

[16] Xiong J, He J, Zhu J, Pan J, Liao W, Ye H, et al. Lactylation-driven METTL3-mediated RNA m^6A modification promotes immunosuppression of tumor-infiltrating myeloid cells. Molecular Cell. 2022; 82: 1660–1677.e10. https://doi.org/10.1016/j.molcel.2022.02.033

[17] Li X, Xu X, Zhang Q, Ling M, Li X, Tan X. METTL14 promotes fibroblast-like synoviocytes activation via the LASP1/SRC/AKT axis in rheumatoid arthritis. American Journal of Physiology. Cell Physiology. 2023; 324: C1089–C1100. https://doi.org/10.1152/ajpcell.00575.2022

[18] Zhuang T, Chen MH, Wu RX, Wang J, Hu XD, Meng T, et al. ALKBH5-mediated m6A modification of IL-11 drives macrophage-to-myofibroblast transition and pathological cardiac fibrosis in mice. Nature Communications. 2024; 15: 1995. https://doi.org/10.1038/s41467-024-46357-x

[19] Chen Y, Wan R, Zou Z, Lao L, Shao G, Zheng Y, et al. O-GlcNAcylation determines the translational regulation and phase separation of YTHDF proteins. Nature Cell Biology. 2023; 25: 1676–1690. https://doi.org/10.1038/s41556-023-01258-x

[20] Ping S, Ye T, Chenjing W, Xin L, Yanping L, Yu C. Celecoxib regulates miR-129-5p/HMGB1 to inhibit the secretion of inflammatory factors in fibroblast-like synovial cells of rheuma-

toid arthritis induced by TNF-α. Chinese Journal of Comparative Medicine. 2022; 32: 82–89.

[21] Noack M, Miossec P. Effects of Methotrexate Alone or Combined With Arthritis-Related Biotherapies in an *in vitro* Coculture Model With Immune Cells and Synoviocytes. Frontiers in Immunology. 2019; 10: 2992. https://doi.org/10.3389/fimmu.2019.02992

[22] Cui LG, Zhai MM, Yin JJ, Wang ZM, Wang SH, Zhou YJ, et al. Targeting the ALKBH5-NLRP3 positive feedback loop alleviates cardiomyocyte pyroptosis after myocardial infarction. European Journal of Pharmacology. 2025; 989: 177247. https://doi.org/10.1016/j.ejphar.2024.177247

[23] Jang S, Kwon EJ, Lee JJ. Rheumatoid Arthritis: Pathogenic Roles of Diverse Immune Cells. International Journal of Molecular Sciences. 2022; 23: 905. https://doi.org/10.3390/ijms23020905

[24] Lu J, Hao J, Zheng J, Liao H, Liu C, Shen H. IL-25 Attenuates Rheumatoid Arthritis via Inhibition of the TLR4/NF-κB/NLRP3 Signaling Pathway. Discovery Medicine. 2025; 37: 2687–2701. https://doi.org/10.24976/Discov.Med.202537202.225

[25] Teng Y, Yin H, Feng R, Jiang L, Qiu W, Duan X, et al. Methotrexate inhibits glucocorticoids-induced osteoclastogenesis via activating IFN-γR/STAT1 pathway in the treatment of rheumatoid arthritis. RMD Open. 2024; 10: e004886. https://doi.org/10.1136/rmdopen-2024-004886

[26] Kansal R, Sharma V, Potraje P, Datta M. m6A RNA modification and its emerging roles in diseases: recent advances and therapeutic implications. Journal of Translational Medicine. 2026; 24: 433. https://doi.org/10.1186/s12967-026-07805-y

[27] Aihaiti Y, Song Cai Y, Tuerhong X, Ni Yang Y, Ma Y, Shi Zheng H, et al. Therapeutic Effects of Naringin in Rheumatoid Arthritis: Network Pharmacology and Experimental Validation. Frontiers in Pharmacology. 2021; 12: 672054. https://doi.org/10.3389/fphar.2021.672054

[28] Wei G. RNA m6A modification, signals for degradation or stabilisation? Biochemical Society Transactions. 2024; 52: 707–717. https://doi.org/10.1042/BST20230574

[29] Zhou H, Shen X, Yan C, Xiong W, Ma Z, Tan Z, et al. Extracellular vesicles derived from human umbilical cord mesenchymal stem cells alleviate osteoarthritis of the knee in mice model by interacting with METTL3 to reduce m6A of NLRP3 in macrophage. Stem Cell Research & Therapy. 2022; 13: 322. https://doi.org/10.1186/s13287-022-03005-9

[30] Williamson J, Petralia RS, Wang YX, Mattson MP, Yao PJ. Purine Biosynthesis Enzymes in Hippocampal Neurons. Neuromolecular Medicine. 2017; 19: 518–524. https://doi.org/10.1007/s12017-017-8466-6

[31] Mumtaz T, Tahir A, Tariq MA, Iqbal MA. Comparative analysis of multiorgan toxicity induced by long term use of disease modifying anti-rheumatic drugs. PloS One. 2023; 18: e0290668. https://doi.org/10.1371/journal.pone.0290668

[32] Liu L, Yan YD, Shi FH, Lin HW, Gu ZC, Li J. Comparative efficacy and safety of JAK inhibitors as monotherapy and in combination with methotrexate in patients with active rheumatoid arthritis: A systematic review and meta-analysis. Frontiers in Immunology. 2022; 13: 977265. https://doi.org/10.3389/fimmu.2022.977265